

MIT Open Access Articles

*Silver nanoparticle structures realized
by digital surface micromachining*

The MIT Faculty has made this article openly available. **Please share** how this access benefits you. Your story matters.

Citation: Lam, E.W., H. Li, and M.A. Schmidt. "Silver nanoparticle structures realized by digital surface micromachining." Solid-State Sensors, Actuators and Microsystems Conference, 2009. TRANSDUCERS 2009. International. 2009. 1698-1701. ©2009 Institute of Electrical and Electronics Engineers.

As Published: <http://dx.doi.org/10.1109/SENSOR.2009.5285759>

Publisher: Institute of Electrical and Electronics Engineers

Persistent URL: <http://hdl.handle.net/1721.1/59526>

Version: Final published version: final published article, as it appeared in a journal, conference proceedings, or other formally published context

Terms of Use: Article is made available in accordance with the publisher's policy and may be subject to US copyright law. Please refer to the publisher's site for terms of use.



SILVER NANOPARTICLE STRUCTURES REALIZED BY DIGITAL SURFACE MICROMACHINING

*E.W. Lam**, *H. Li*, and *M.A. Schmidt*

Microsystems Technology Laboratories
Massachusetts Institute of Technology, Cambridge, Massachusetts, USA

ABSTRACT

We report a new surface micromachining process using commercial silver nanoparticle inks and digital fabrication methods. This process is entirely digital (non-lithographic patterning), the feature sizes can be $<20\mu\text{m}$, and the maximum temperature is less than 250°C . Furthermore, we have completed materials property characterization in order to enable design in this process. As a demonstration, silver cantilevers were fabricated using this process and subsequently characterized to determine the silver film's mechanical properties.

KEYWORDS

MEMS, Inkjet, Printing, Nanoparticles

INTRODUCTION

To date, MEMS devices have typically been realized using the semiconductor industry's manufacturing methods. While these methods are well suited for high-volume products realized using standardized processes, they can impose severe technical and economic constraints on lower volume and/or large area products. In this work, we seek to develop alternative MEMS manufacturing methods that offer the promise of extremely low cost/area in low volume. The principle tool we exploit towards this goal is thermal inkjet (TIJ) printing, which has of course realized low cost/area in digital photography. This method is one of several techniques that fall in the category of *digital fabrication*. These techniques encompass a wide variety of methods including laser-writing, inkjet deposition, and electrochemical deposition [1].

Previous work in this field demonstrated the feasibility of using inkjet printing for fabricating MEMS devices including MEMS electric motors and heat actuators or "heatuators" [2]. However, even though working devices were fabricated, the devices were large, on the order of millimeters with the smallest feature sizes of $\sim 100\mu\text{m}$, limiting the potential applications. Additionally, mechanical properties of the devices were not reported.

Using Hewlett-Packard (HP) thermal inkjet (TIJ) technology mounted to an X-Y microcontroller stage, we present a digital surface micromachining process flow with a 250°C thermal budget. The process uses Cabot Corporation's silver-based conductive ink for the structural layer and PMMA ink for the sacrificial layer. We explored several parameters for optimization including drying environment and sintering conditions to reliably control

and predict the resulting shape, size, and quality of the printed structures. These optimized parameters were used to fabricate silver cantilevers and structures with features down to $20\mu\text{m}$. The cantilevers were used to characterize the mechanical properties of the silver.

PROCESS OVERVIEW

The fabrication process contains eight steps as summarized in Figure 1. The sacrificial layer is jetted and planarized. An additional sacrificial feature is deposited around the step to serve as a barrier to contain the silver ink while it dries and sinters. The silver ink is jetted into the sacrificial "mold" and is sintered to form a self-supporting film. The structures are laser-trimmed to remove the undesirable features, such as the film that partially coats the barrier (shown in Figure 1, step 6). The resulting structures are then released to complete the surface micromachining process. Figure 2 is an SEM image of a printed silver cantilever.

APPARATUS

Fluidic deposition is controlled by a HP Thermal Inkjet Pico-fluidic System (TIPS). The TIPS consists of an electronic controller and replaceable 0.5mL print cartridges. At the end of each cartridge is a small TIJ printhead that dispenses 2pL-220pL, depending on the TIJ nozzle size, which lead to spot sizes as low as $25\mu\text{m}$. Coupled with the TIPS is a back pressure controller that monitors the amount of vacuum the reservoir experiences and ultimately determines the amount of ink delivered to the TIJ nozzle.

The TIPS is attached to a XY Galil microcontroller with $1\mu\text{m}$ step resolutions. The microcontroller is complimented by a visual alignment system for fabricating multi-layer devices. The microcontroller maneuvers over a heated platen that has a maximum temperature of $\sim 120^\circ\text{C}$. The nozzle is typically suspended 1mm above the substrate and has a drop placement accuracy of $\pm 3\mu\text{m}$ on the substrate.

MATERIALS

This process has three layers/materials: substrate, sacrificial layer, and structural layer. While this process is compatible with multiple substrates, a glass substrate was chosen for compatibility with the circuitry process that will ultimately be incorporated with these structures.

The sacrificial layer is created from poly-(methyl

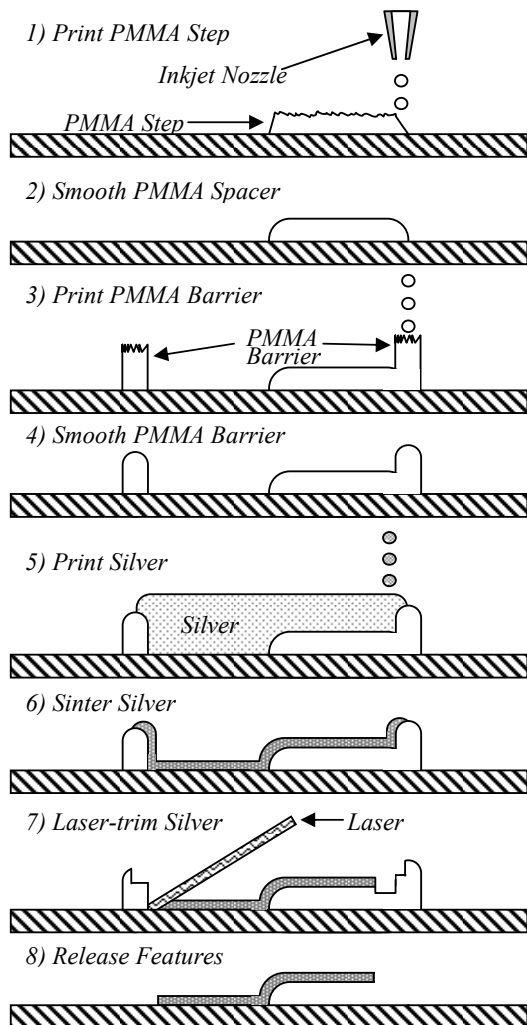


Figure 1. Digital Fabrication Silver Surface Micromachining Process Flow. Steps 3-4 and 7 are optional but result in better feature definition.

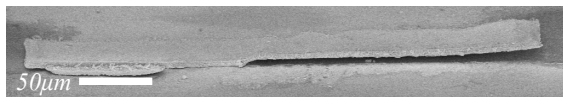


Figure 2. SEM image of surface micromachined cantilevers. The variation in gap is caused by non-uniform spacer thickness.

methacrylate) (PMMA) dissolved in toluene. After considering and experimenting with several other materials, including Aluminum tris-(8-hydroxyquinoline), photoresist, and ZnO nanoparticles, we determined that the PMMA ink had the best combination of chemical and thermal compatibility with the structural (silver) ink.

The structural ink is Cabot Corporation's silver-based conductive ink. This ink contains 30nm silver nanoparticles coated with a thin ligand shell to prevent aggregation and is suspended in an ethylene glycol/ethanol solution. Films made from this ink become electrically conductive after a thermal sintering at temperatures greater than 120°C. To make this ink more readily printable, the

ink's viscosity was lowered by diluting 1:2 volumetrically with ethanol.

INKJET DEPOSITION

Prior to printing, the droplet diameters for the PMMA and silver inks were characterized to improve fabrication reliability and film uniformity. The PMMA ink used an 80pL TIJ nozzle and had a droplet diameter of 120µm while the silver used a 35pL TIJ nozzle and droplet diameter was 80µm. The PMMA ink required a larger nozzle because its higher viscosity prevented reliable printing using smaller nozzles. During deposition the platen was isothermally held at 40°C to assist in ink drying and prevent ink running. While the reservoir was not heated, due to its proximity to the platen the nozzle was consistently at 38°C-40°C.

SOLVENT VAPOR ANNEALING

The PMMA layers require post-deposition processing to form uniform features. Because of toluene's volatility, the as-deposited PMMA features are cracked and non-uniform. To mend these features, the samples are placed into containers filled with solvent (toluene or acetone) vapors. These vapors lower the PMMA's glass-transition temperature and cause the PMMA to reflow, or partially melt, at room temperature [3]. This partial melting enables the PMMA to repair itself, filling in cracks and smoothing out non-uniformities (Figure 3). Because the smoothness and uniformity of the PMMA spacer is critical, the devices are kept in the solvent vapor container for 10 minutes for step 2. Additionally, to prevent the PMMA barrier and spacer from merging together, the solvent vapor anneal in step 4 is limited to 3 minutes.

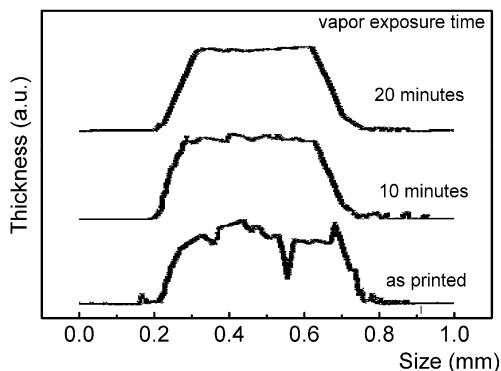


Figure 3. Smooth and flat PMMA feature by inkjet printing and sequential solvent annealing steps. (Courtesy of Dr. Jianglong Chen - MIT)

SILVER FILM PROCESSING

There are two important parameters in forming the silver films: drying and sintering. Drying is important in preventing crack formation: by lowering the evaporation rate we are able to reduce the capillary forces, preventing stress buildup inside the films, and prevent cracking. Sintering drives silver nanoparticles fusion and influences

the film's nanostructure, including grain growth and film porosity. The nanostructure strongly influences the film's final mechanical properties.

Drying Silver Films

Silver films were jetted directly onto glass substrates and hotplate-, tube furnace- (filled with N₂), or vacuum-dried. Samples were considered dry when the films became metallic and reflective (originally the films are dull and purple). The hotplate and tube furnace samples were isothermally held at 80°C until the samples were dried (~3 hours and ~18 hours, respectively). The vacuum-dried sample was kept at 10⁻²torr for 1 hour at room temperature. Cracking was observed in the hotplate- and vacuum dried samples while the tube furnace-dried sample exhibited virtually no cracking (Figure 4). It is believed that the rate of drying is primarily responsible for crack formation, as the drying rate was lowest in the tube furnace when the N₂ flow rate is minimized.

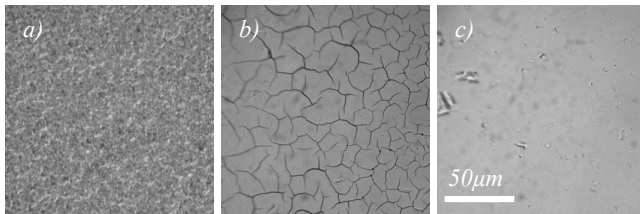


Figure 4. Optical micrographs of a) vacuum-, b) hotplate-, and c) tube furnace-dried samples. Apparent roughness in a) are microcracks.

Sintering Silver Films

Cabot silver films were printed directly onto glass substrates and both dried and sintered in a tube furnace at peak temperatures of 150-400°C. The samples were ramped up to the peak temperature at 1.5°C·min⁻¹, isothermally held for 30 minutes, and then ramped down to room temperature at 1.5°C·min⁻¹ in a N₂-filled tube furnace. Figure 5 show the resulting SEM images of the silver films. As expected, we see an increase in grain size with increasing sintering temperature. The silver films

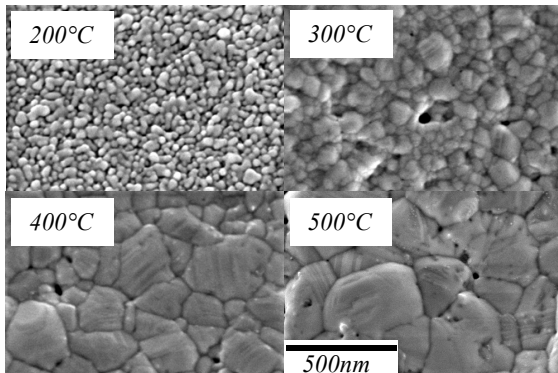


Figure 5. SEM images of Cabot silver films taken at same magnification. The film's nanostructure significantly changes as sintering temperature increases.

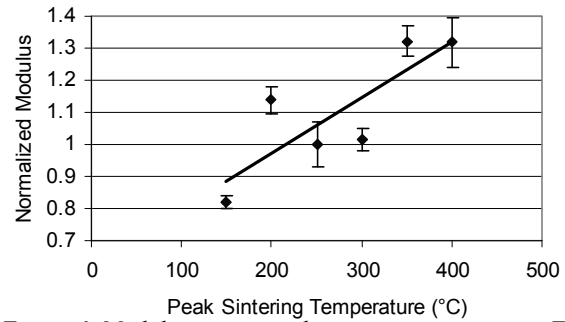


Figure 6. Modulus versus peak sintering temperature. The moduli were obtained by nanoindenting Cabot silver films.

were also nanoindented and display a correlating increase in modulus as depicted in Figure 6.

Additional Cabot silver samples printed on glass were prepared and sintered on a hotplate (in air), a vacuum furnace, and in a N₂-filled tube furnace. The tube furnace and hotplate were heated with 3°C·min⁻¹ ramp up/down with an isothermal hold at 150°C for three hours. The vacuum oven's temperature was increased 25°C every 10 minutes and held at 150°C for 3 hours. The samples were nanoindented to determine the films' Young's moduli (Figure 7). The results suggest sintering environment plays a significant role in the final mechanical properties.

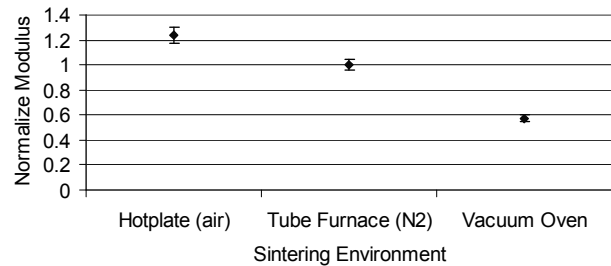


Figure 7. Normalized Modulus versus sintering environment. Moduli were obtained by nanoindentation.

Process of Record

In the final process the silver is dried and sintered in a tube furnace filled with N₂. The tube furnace is ramped up to 250°C at 1.5°C·min⁻¹ and is isothermally held at 250°C for 30 minutes. The tube furnace is then cooled to room temperature at the same ramp rate of 1.5°C·min⁻¹. The drying was merged with the sintering because it was observed that the film dried faster at elevated temperatures while still remaining crack-free.

LASER TRIMMING

A Resonetics laser milling tool is used to remove any undesired features and artifacts. In addition to random artifacts caused by stray droplets, debris, etc., there is a large undesired rim formed around the features formed by the PMMA barriers. Laser trimming define finer features such as the pinholes and tethers as shown in Figure 8.

RELEASING FEATURES

The final step is releasing the structures by removing the spacer. The structures are placed in 15-, 10-, and 5-minute chloroform baths and then dried using an N₂ gun. Stiction has been observed in several cases; however this stiction can be overcome by mechanical methods or rinse optimization.

RESULTS AND CHARACTERIZATION

As a demonstration of the process, we fabricated a pinwheel accelerometer proof mass as shown in the SEM images in Figure 8. This proof mass contains multiple 50 μ m x 50 μ m pinholes to show its capability to pattern well-defined relief structures. We typically use structural layer thicknesses of 3 μ m and spacer layer thicknesses of 2.5 μ m, but other thicknesses are possible.

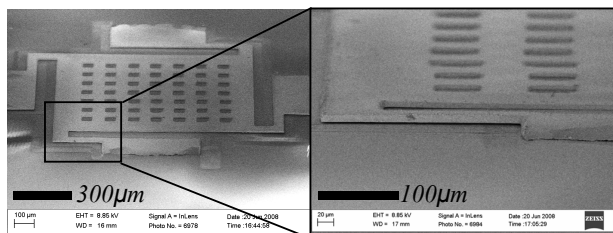


Figure 8. Pinwheel accelerometer structure realized by digital surface micromachining.

Cantilevers of dimensions 200 μ m (length) and 50 μ m or 100 μ m (width) were fabricated for characterization purposes. Using a Tencor P-10 contact profilometer, known force loads were applied to the cantilevers and the resulting mechanical deflections were measured. These force-deflection measurements were used to determine the silver's elastic modulus of 21.9 \pm 1.50GPa. This value was calculated assuming the film has uniform thickness and the beam thickness and the anchor thickness were the same. The anchor thicknesses were measured using contact profilometry.

The measurements were repeated using a Hysitron nanoindenter. Using a series of point-force deflection measurements (Figure 9) and the assumed cantilever beam thickness, the silver's elastic modulus was confirmed to be 22 \pm 1.5GPa. These results are consistent with measurements made by nanoindenting anchors of silver cantilevers that were directly printed on glass. This measured modulus is significantly lower than bulk silver's modulus (83GPa). We believe this difference is a result of the nanostructure of the film, which is consistent with the observed grain size versus modulus data of Figures 5 & 6.

CONCLUSIONS

In summary, we presented a new surface micromachining process that uses a commercial silver nanoparticle ink capable of feature sizes <20 μ m and maximum temperature less than 250 $^{\circ}$ C. We used this to

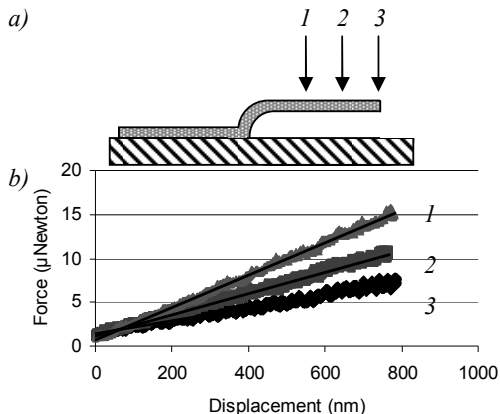


Figure 9. Point-force deflection measurements used to mechanically characterize the cantilever. The elastic modulus is 22 \pm 1.5GPa.

fabricate pinwheel accelerometer proof masses and cantilevers. The cantilevers were mechanically characterized and we determined the Young's modulus to be 22 \pm 1.5GPa. These measurements were consistent with values determined by nanoindenting silver films directly printed on glass. The measured modulus is significantly lower than bulk silver's modulus, which we believe is a result of the nanostructure of the film. Investigations of varying sintering temperatures and environments support this hypotheses and offer suggestions on further silver film improvement and process optimizations.

ACKNOWLEDGEMENTS

This work is sponsored by DARPA N/MEMS Fundamentals Program and HP. We thank HP for the loan of the TIPS devices. TIPS is a prototype laboratory device used internally at HP and with selected research partners. We would also like to acknowledge Dr. Jianglong Chen, Dr. Valerie Leblanc, and Professor Vladimir Bulović for their assistance in using the TIPS devices and development of the solvent vapor annealing technique.

REFERENCES

- [1] S. Roy, "Fabrication of micro- and nano-structured materials using mask-less processes", *J. Phys. D: Appl. Phys.*, vol. 40, pp. R413-R426, 2007.
- [2] S.B. Fuller, E.J. Wilhelm, J.A. Jacobson, "Ink-jet printed nanoparticle micromechanical systems", *J. Microelectromech. Syst.*, vol. 11, pp. 54-60, 2002.
- [3] J. Feng, M. Winnik, R.R. Shivers B. Clubb, "Polymer Blend Latex Films: Morphology and Transparency", *Macromolecules*, vol. 28, pp. 7671-6782, 1995.
- [4] D. Soltman, V. Subramanian, "Inkjet-Printed Line Morphologies and Temperature Control of the Coffee Ring Effect", *Langmuir*, vol. 24, pp. 2224-2231, 2008.

CONTACT

* E.W. Lam, tel: +1-617-253-0224; EWLAM@MIT.edu